Phonon sidebands and optical gain of light-emitting conjugated polymers

Hsin-Fei Meng*

Institute of Physics, National Chiao Tung University, Hsinchu 300, Taiwan, Republic of China

Vincent Chia-Hung Chang[†]

Department of Physics, National Taiwan Normal University, Taipei 116, Taiwan, Republic of China
and National Center for Theoretical Sciences, Hsinchu 300, Taiwan, Republic of China

We study the interaction of excitons and optical phonons in light-emitting conjugated polymers with the variational approach. The optical transition matrix elements for the phonon sidebands in the absorption and emission spectra are calculated. The electron-phonon coupling constant is determined by fitting the theoretical oscillator strengths of the emission sidebands with the experimental photoluminescence spectra for the various poly(p-phenylene vinylene) derivatives. Using this coupling constant, we predict that the absorption one-phonon sideband is as important as the zero-phonon sideband for the ideal systems. Taking the experimental data of the peak absorption coefficient as input, we obtain the optical gain coefficient for a wide range of exciton densities. The gain is found to be determined by the exciton density n_0 by a general expression $1.98 \times 10^{-16} n_0$ cm^2, which is in good agreement with experiments. [S0163-1829(99)06243-8]

I. INTRODUCTION

Conjugated polymer has been identified as a promising candidate for future optoelectronic applications[1]. Encouraged by the discovery of their electroluminescence,[2] an enormous amount of research has been conducted to further explore the possibilities of electro-optical devices based on conjugated polymers. A nature step forward is the search for lasing actions. Preliminary optically pumped polymer lasers have been demonstrated.[3–6] The effort to develop these prototypes into realistic coherent light sources with preferably electrical pumping has, however, encountered major difficulties. In order to solve these difficulties, more works need to be done on not only the technical issues such as device fabrications, but also the basic physics of lasing mechanisms in conjugated polymers. This paper is motivated by the latter.

Lasing takes place when the gain overcomes the loss in an optical resonator. For gas lasers with typical three or four-level operation, gain is achieved by the population inversion between the two active levels. Due to the inversion, the rate for the absorption from the lower state is smaller than the rate of stimulated emission from the upper state. In the case of inorganic semiconductor lasers, gain occurs between two bands of extended states, i.e., the conduction band and the valence band, instead of two discrete active states. Upon current injection, the conduction-band bottom is occupied by the electrons and the valence-band top is occupied by holes. Absorption near the band edge is then depleted, while stimulated emission is enhanced at the same time. In other words, the current injection causes a spectral shift between the absorption and the emission, which grows with the carrier density and therefore injection current. As a result, net gain arises. Though conjugated polymers are also direct band-gap semiconductors, which exhibit gain upon pumping, the scenario for gain seems to be quite different from above. One of the most important differences is that even before optical pumping or current injection, a significant spectral shift be-

tween the absorption and emission, i.e. Stokes shift, exists for conjugated polymers. Due to this shift, the emitted photon has a reduced chance to be reabsorbed and the optical gain is possible without electronic population inversion. The Stokes shift, common in organic materials, is usually due to the electron-phonon coupling, which causes vibrational relaxations after electronic excitations. With the Stokes shift, lasing can occur without electronic population inversion, in contrast to the conventional compound semiconductors.

In this paper, we study theoretically the phonon sidebands in the absorption and emission spectra and the resulting Stokes shift due to electron-lattice coupling for one idealized infinite periodic chain. The significance of extrinsic factors like the inhomogeneity broadened density of states (DOS) will be investigated afterwards. The theory developed by Pollmann, Buttner, and Matsurra[7,8] (PBM) for polar inorganic semiconductors is adapted for the description of conjugated polymers. Besides dimensionality, one of the major differences between conjugated polymers and polar semiconductors is the type of the electron-phonon coupling. While the coupling for polar semiconductors is of the Fröhlich type, the coupling for the covalently bonded conjugated polymers is of deformation nature.

If the oscillator strength of the absorption is not dominated by the zero-phonon band, there will be a subsequent relaxation among the vibrational levels from the higher phonon states to the zero-phonon state after optical excitation. Such a relaxation is sometimes referred to as the genuine Stokes shift. This shift reduces the overlap between the emission and the absorption spectra, and favors the achievement of gain. We predict that for ideal systems the oscillator strength of the absorption is evenly shared by the one- and zero-phonon band, while the emission is dominated by the zero-phonon band. The mirror symmetry common for small organic molecules is therefore broken. Moreover, this result implies the possibility of a genuine Stokes shift of one optical phonon energy, contrary to the interpretations of some

site-selective experiments.[9,10] We shall come back to this point in the Discussion.

Because our calculation is only for one single chain, the absorption and emission coefficient for a realistic solid-state sample can be determined only up to a common proportional constant, which includes factors like transition dipole matrix element and chain packing density. We determine the constant from fitting with the experimental absorption coefficient, then calculate the gain coefficient for arbitrary exciton density. We found that near the one-phonon emission band there is a universal relation between the peak gain coefficient and the exciton volume density, independent of the chain packing density and geometry. This result gives a relation between the resonator loss and the threshold exciton density required for lasing in practical resonators. The agreement with the experimental estimates is quite reasonable.

This article is organized as follows: In Sec. II, we present our model Hamiltonian and the Lee-Low Pines (LLP) unitary transformation. In Sec. III, the variational approach to derive the wave functions and energy is introduced. In Sec. IV, we calculate the optical transition matrix elements and present our results on the absorption and emission spectra with phononside bands. In Sec. V, we study the gain coefficient for arbitrary exciton density and compare the theoretical predictions with experiments. Sections VI and VII are the discussion and the conclusion, respectively.

II. THE EXCITON-PHONON HAMILTONIAN

Poly(p-phenylenevinylene) (PPV) is idealized as an one-dimensional lattice. Each unit cell contains eight carbon atoms, with one p_z orbital at each carbon atom. The π-electron bands are formed by the superposition of these p_z orbitals. The total number of π electrons is equal to the total number of carbon atoms. Simple tight-binding calculation shows that PPV is a direct band-gap semiconductor. Because optical absorption and emission near the band gap involve transitions between the valence and the conduction bands only, the problem can be simplified from eight bands to only two bands. The system then consists of an electron and a hole interacting with each other and with the longitudinal-optical phonons. It is convenient to write an effective Hamiltonian for the system

$$H = H_{ex} + H_p + H_{ex-p}, \qquad (1)$$

with

$$H_{ex} = \frac{p_e^2}{2m_e} + \frac{p_h^2}{2m_h} + V(r_e - r_h) \qquad (2)$$

and

$$H_p = \sum_{s=1}^{n} \sum_{k} \omega_s(k) a_{s,k}^\dagger a_{s,k}. \qquad (3)$$

The three terms in H are for the electron-hole system of exciton, phonon, and their interaction, respectively. H_{ex-p} will be derived below. $p_{e(h)}$ is the momentum operator for electron (hole). $m_{e,h}$ are the effective mass of the conduction and valence bands, respectively. $V(r)$ is the effective Coulomb attraction between the electron and the hole. s is the

phonon branch index, and k is the crystal momentum. The π-electron band edge is chosen to be at $k=0$. $a_{s,k}^\dagger$ and $a_{s,k}$ are the phonon creation and annihilation operators, respectively.

In contrast to the Fröhlich type coupling in polar semiconductors, the electron-phonon coupling in conjugated polymers are of deformation nature. Its explicit form can be obtained as follows. Consider the interaction Hamiltonian H_{e-p} between conduction-band electron and phonon first. From the crystal momentum conservation, the matrix element of H_{e-p} between conduction-band Bloch states $|k\rangle$ and $|k'\rangle$ must be of the form

$$\langle k' | H_{e-p} | k \rangle = \sum_{sq} \xi_e^{s,q} (a_{s,q} + a_{s,-q}^\dagger) \delta_{k',k+q}. \qquad (4)$$

For deformation type of interaction, the coupling constant $\xi_e^{s,q}$ approaches to a finite value as $q \to 0$. Since the exciton is composed of Bloch states near the Brillouin zone center, we only need to consider electron scattering in that region, where $\xi_e^{s,q}$ can be replaced by its value at $q=0$, denoted simply by ξ_e^s below. In fact, from the relation $\langle k | H_{e-p} | k \rangle = \xi_e^s (a_{s,0} + a_{s,0}^\dagger)$, ξ_e^s is identified to be the change of the conduction-band edge due to the $q=0$ mode of the lattice displacement with normal coordinate $\chi_{s,q}$, which is equal to $(a_{s,q} + a_{s,q}^\dagger)/\sqrt{2}$ in the second quantized form. The lattice displacement vector $\mathbf{u}_s^i(R)$ for the ith carbon atom in the nth unit cell can be expressed in terms of the normal coordinate $\chi_{s,q}$ by

$$\mathbf{u}^i(R_n) = \sqrt{\frac{1}{N}} \sum_{q,s} \sqrt{\frac{\hbar}{2M_c \omega_s(q)}} \boldsymbol{\epsilon}_s^i(q) e^{iqR_n} \sqrt{2} \chi_{s,q}. \quad (5)$$

N is the total number of unit cells in the chain. R_n is the location of the nth unit cell. M_c is the mass of the carbon atom. $\boldsymbol{\epsilon}_s^i(q)$ are the polarization vectors. $i = 1 \to 8$ label the carbon atoms in each unit cell. The dependency of the conduction-band edge ε_c on $\chi_{s,0}$ is through the modulation of the hopping integral between neighboring carbon p_z orbitals by the lattice displacement. Assume that α is the change in the hopping integral per unit length of the bond-length change. The bond-length change is of the order of $|\mathbf{u}^i|$, which is in turn of the order of $\sqrt{\hbar/2NM_c \omega_s(q)}$, so we have

$$\xi_e^s = \frac{\partial \varepsilon_c}{\partial \chi_{s,0}} \sim \alpha \sqrt{\frac{\hbar}{2NM_c \omega_0}}, \qquad (6)$$

assuming that all the phonon branches are dispersionless and share the same frequency ω_0. This relation gives only the correct order of magnitude for the electron-phonon coupling constant ξ_e^s. The exact expression for ξ_e^s depends on the polarization vectors $\epsilon_s^i(q)$ of the phonon modes. Instead of solving the complete lattice dynamic equation to obtain all the polarization vectors, we introduce a phenomenological dimensionless parameter η_e, and assume that the coupling constant ξ_e^s is independent of the branch index s, by

$$\xi_e^s = \xi_e = \eta_e \alpha \sqrt{\frac{\hbar}{2NM_c \omega_0}}. \qquad (7)$$

η_e represents the strength of the electron-phonon coupling. Similarly, for the valence band we can calculate the modulation of the valence-band edge by the lattice displacement of the normal phonon modes $\chi_{s,q}$, and obtain the corresponding hole-phonon coupling constant ξ_h. The lattice structure of PPV is invariant under inversion respect to the center of the benzene ring. Therefore, the set of eight polarization vectors $\epsilon^i_{s,q}$ for each mode (s,q) must be either even or odd upon inversion. The energies of the electronic bands at $q=0$ is actually the eigenvalues of a 8×8 symmetric matrix A, with A_{ij} equal to the hopping integral between carbon site i and j. A is invariant upon lattice inversion when the lattice is in the equilibrium configuration. When the lattice is displaced from the equilibrium configuration, the matrix is modulated $A\rightarrow A+\Delta A$. One can show that for even polarization vectors, ΔA is odd upon lattice inversion. On the other hand, ΔA is even upon lattice inversion for odd polarization vectors. There is a bandedge modulation to the linear order in the displacement only when ΔA is even. Moreover, we found that for such ΔA, the modulation of the conduction band and the valence band are always exactly the same in size but opposite in sign. Therefore, we have the general relation $-\xi_v=\xi_e\equiv\xi$. However, because hole is the vacancy of the valence band, the matrix elements between the one-hole states are opposite in sign to the matrix elements of the corresponding valence-band states. In other words, we have $_h\langle k'|H_{h-p}|k\rangle_h=-_v\langle k'|H_{h-p}|k\rangle_v$ up to a constant. Here, $|k\rangle_v$ is the one-body valence-band Bloch state, while $|k\rangle_h$ is the many-body Slater determinant with one hole in the otherwise filled valence band. So we have $\xi_h=-\xi_v=\xi$. Finally in the real-space representation, the exciton-phonon interaction Hamiltonian becomes

$$H_{ep-p}=H_{e-p}+H_{h-p}=\sum_{sk}\xi(e^{iqr_e}+e^{iqr_h})(a_{s,q}+a^\dagger_{s,-q}),$$
(8)

with

$$\xi=\eta\alpha\sqrt{\frac{\hbar}{2NM_c\omega_0}}.$$
(9)

$r_{e,h}$ are the one-dimensional coordinates of the electron and hole, respectively. In this interaction Hamiltonian, η is the only fitting parameter.

Expressed in terms of the center-of-mass and relative coordinates of the exciton, the total Hamiltonian becomes

$$H=\frac{P^2}{2M}+\frac{p^2}{2\mu}+\hbar\omega_0\sum_{s,k}a^\dagger_{s,k}a_{s,k}$$
$$+\sum_{s,k}\xi[e^{ikR}\rho_k(r)a_{s,k}+\text{h.c.}]+V(r).$$
(10)

Here $M=m_e+m_h$ is the total mass, $\mu=m_em_h/M$ is the reduced mass. $R=r_e+r_h$ is the center-of-mass coordinate, and $r=r_e-r_h$ is the relative coordinate. $\rho_k(r)$ is defined as

$$\rho_k(r)\equiv\exp(is_2kr)+\exp(is_1kr)$$
(11)

with the ratio $s_1=m_e/M$ and $s_2=m_h/M$. Next, we perform the Lee-Low-Pines (LLP) transformation[11] to remove the center-of-mass degree of freedom

$$H_1\equiv U^{-1}_1HU_1,U_1=\exp\left[i\left(Q-\sum_{s,k}ka^\dagger_{s,k}a_{s,k}\right)R\right].$$
(12)

The transformed Hamiltonian becomes

$$H_1=\frac{\hbar^2Q^2}{2M}+\frac{p^2}{2\mu}+V(r)+\sum_k\xi[\rho_k(r)a_k+\text{H.c.}]$$
$$+\sum_k\hbar\tilde{\Omega}(k,Q)a^\dagger_ka_k+\sum_{k,k'}\frac{\hbar^2kk'}{2M}a^\dagger_ka^\dagger_{k'}a_ka_{k'},$$
(13)

with

$$\hbar\tilde{\Omega}(k,Q)\equiv\hbar\omega_0-\frac{\hbar^2kQ}{M}+\frac{\hbar^2k^2}{2M}.$$
(14)

Q is the total momentum of the system, which is conserved and taken as a c number here. Note that we have included the summation over the phonon branch index s into the summation over wave number k implicitly.

This Hamiltonian is of similar form with the exciton-phonon Hamiltonian for conventional three-dimensional polar inorganic semiconductors studied by PBM.[7,8] In addition to dimensionality, there are two major differences between the Hamiltonians for conjugated polymers and polar semiconductors. First the k dependency of the coupling constant is different. The coupling is a constant for the polymers, but proportional to $1/k$ for the polar semiconductors. Second, the electron-phonon coupling and hole-phonon coupling in $\rho_k(r)$ have the same sign for polymers, but different in polar semiconductors.

III. VARIATIONAL SCHEME

Following the work of PBM, the trial ground state $|\Psi\rangle$ of the whole system is chosen to be of the form

$$|\Psi\rangle=\phi_{ex}(r)U_2[F_k(r)]|0\rangle_{ph}.$$
(15)

$\phi_{ex}(r)$ is the exciton trial wave function. $|0\rangle_{ph}$ is the phonon ground state. U_2 is a displacement operator such that the phonon trial ground state is a coherent state

$$U_2[F_k(r)]=\exp\left[\sum_kF^*_k(r)a_k-F_k(r)a^\dagger_k\right].$$
(16)

$F_k(r)$ is our variational function. We define

$$H_2\equiv U^{-1}_2[F_k(r)]H_1U_2[F_k(r)],$$
(17)

and

$$H_0\equiv{}_{ph}\langle0|H_2|0\rangle_{ph},$$
(18)

such that the trial ground-state energy $\langle\Psi|H_1|\Psi\rangle$ is equal to $\langle\phi_{ex}|H_0[F_k(r)]|\phi_{ex}\rangle$. The variational ground state is determined by the minimum conditions

$$\frac{\delta}{\delta F_k(r)}\langle\phi_{ex}|H_0[F_k(r)]|\phi_{ex}\rangle=0 \quad (I),$$

$$\frac{\delta}{\delta\phi_{ex}(r)}\langle\phi_{ex}|H_0[F_k(r)]|\phi_{ex}\rangle=0 \quad (II). \quad (19)$$

Due to the translational symmetry of the system, the phonon variational function should be of the form[12]

$$F_k(r)=\frac{\xi}{\hbar\omega_0}(f_k^1 e^{is_2 kr}-f_k^2 e^{is_1 kr}). \quad (20)$$

So the first of the two minimum conditions is replaced by

$$\frac{\delta}{\delta f_k^i}\langle\phi_{ex}|H_0|\phi_{ex}\rangle=0. \quad (21)$$

A. Phonon displacement trial functions

We proceed with condition I in Eq. (19) first. For given exciton trial wave function $\phi_{ex}(r)$, condition I gives the phonon trial functions $F_k(r)$ as functionals of ϕ_{ex}. In terms of f_k^i, the minimum condition becomes

$$\frac{\delta}{\delta f_k^i}\langle\phi_{ex}|H_0|\phi_{ex}\rangle=\langle\phi_{ex}|\frac{\delta F_k(r)}{\delta f_k^i}\frac{\delta}{\delta F_k(r)}H_0|\phi_{ex}\rangle=0. \quad (22)$$

Assuming the inversion symmetry of the exciton wave function $\phi_{ex}(r)=\phi_{ex}(-r)$, the equations can be solved

$$f_k^1=\frac{(1+G_k)(1+R_2^2 k^2)-(1+G_k)G_k}{(1+R_1^2 k^2)(1+R_2^2 k^2)G_k^2},$$

$$f_k^2=\frac{-(1+G_k)(1+R_1^2 k^2)+(1+G_k)G_k}{(1+R_1^2 k^2)(1+R_2^2 k^2)-G_k^2}, \quad (23)$$

where $G_k\equiv\langle\phi_{ex}|e^{ikr}|\phi_{ex}\rangle$, and $R_{1,2}\equiv\sqrt{\hbar/2m_{e,h}\omega_0}$ is the so called polaron radius. Note G_k is real due to the symmetry of $\phi_{ex}(r)$. The dependency of the phonon trial function f_k^i on the exciton trial wave function $\phi_{ex}(r)$ is now only through the quantity G_k. We now substitute Eq. (23) into $\langle\phi_{ex}|H_0[F_k(r)]|\phi_{ex}\rangle$, and express the expectation value in terms of G_k

$$\langle\phi_{ex}|H_0|\phi_{ex}\rangle=\langle\phi_{ex}|H_{free}|\phi_{ex}\rangle$$

$$+\mathcal{R}\eta^2\bar{\alpha}^2\delta_0\left[I_1-\frac{\hbar\omega_0}{\mathcal{R}}I_2+I_3\right]. \quad (24)$$

Here, $H_{free}=p^2/2\mu+V(r)$. $I_{1,2,3}$ are certain dimensionless integrals defined below. $a_B=\hbar^2/\mu e^2\epsilon$ is the exciton Bohr radius. $\mathcal{R}$ is the exciton Rydberg $\hbar^2/2\mu a_B^2$. The lattice constant a is written as $\delta_0 a_B$. In addition, we define the dimensionless polaron radius $\bar{R}_i$ as R_i/a_B and the dimensionless electron-phonon coupling constant $\bar{\alpha}$ by

$$\bar{\alpha}=\frac{\alpha}{\hbar\omega_0}\sqrt{\frac{\hbar}{2M\omega_0}}. \quad (25)$$

For the explicit forms of the integrals I_1, I_2, and I_3, the integration variable k is changed to a dimensionless variable $t\equiv ka_B$, such that $f^{1,2}(t)=f_k^{1,2}$. The function $G(t)$ is defined as G_{t/a_B}. The integrals are

$$I_1=\int_{-\infty}^{\infty}\frac{dt}{2\pi}t^2\{[s_2 f^1(t)]^2+[s_1 f^2(t)]^2$$

$$+2s_1 s_2 f^1(t)f^2(t)G(t)\},$$

$$I_2=\int_{-\infty}^{\infty}\frac{dt}{2\pi}[f^1(t)-f^2(t)][1+G(t)], \quad (26)$$

$$I_3=\int_{-\infty}^{\infty}\frac{dt}{2\pi}\left[\frac{\hbar\omega_0}{\mathcal{R}}+\frac{\sigma}{(1+\sigma)^2}t^2\right]$$

$$\times\{[f^1(t)]^2+[f^2(t)]^2-f^1(t)f^2(t)G(t)\}.$$

Here, σ is m_e/m_h. Note the integrals $I_{1,2,3}$ are expressed in terms of the function $G(t)$, which depends only on the exciton trial wave function $\phi_{ex}(r)$. In order to obtain $\langle\phi_{ex}|H_{free}|\phi_{ex}\rangle$ and the integrals $I_{1,2,3}$ in $\langle\phi_{ex}|H_0|\phi_{ex}\rangle$, we need to chose a definite form of the variational exciton wave function $\phi_{ex}(r)$.

B. Exciton trial wave function

Without the electron-phonon coupling, an exciton in the polymer chain can be modeled as a one-dimensional hydrogen atom with Coulomb interaction cut off at small distances. In fact, the binding energy of the one-dimensional hydrogen atom is infinity without a cutoff.[13] Because our two-band effective mass approach is valid only for Bloch states within the first Brillouin zone, the real-space cutoff for the Coulomb interaction is the lattice constant a, whose corresponding momentum-space cutoff is at the Brillouin zone boundary. The corresponding Schrödinger equation is

$$-\frac{\hbar^2}{2\mu}\frac{d^2\phi}{dr^2}+V(r)\phi=E\phi. \quad (27)$$

The cutoff Coulomb potential is

$$V(r)=\begin{cases}-\dfrac{e^2}{\epsilon|r|}, & |r|>a\\[2mm]-\dfrac{e^2}{\epsilon a}, & |r|<a.\end{cases} \quad (28)$$

Here, ϵ is the dielectric constant along the chain. We assume that the main effect of exciton-phonon interaction is to introduce a modified electron-hole Coulomb attraction. So we take the variational trial wave function for $\phi_{ex}(r)$ as the solution of the Schrödinger equation for $V(r)$ with ϵ changed to ϵ_v. The subscript ''v'' means variation. The modified Bohr radius, denoted by a_0 is then

$$a_0=\frac{\hbar^2}{\mu e^2\epsilon_v}. \quad (29)$$

We take a_0 as our variational parameter to minimize the system total energy. Following the work on Loudon, we define three dimensionless variables

$$\delta = \frac{a}{a_0}, \quad \lambda = \sqrt{\frac{2\mu a_0^2}{\hbar^2}|E|}, \quad z = \frac{2r}{\lambda a_0}, \quad (30)$$

and express the solution and energy eigenvalue in terms of them. δ is now our variational parameter. For the ground state, λ and δ are related by the equation

$$\ln\left(\frac{2\delta}{\lambda}\right) + \frac{1}{2\lambda} = 0. \quad (31)$$

In terms of the new variable z, the cutoff length of the Coulomb potential is $z_0 = 2\delta/\lambda$, and the dimensionless ground-state wave function is

$$\psi(z) = \begin{cases} \cos\left[\left(-\frac{1}{4} + \frac{a_0\lambda^2}{4a}\right)^{1/2} z\right], & z < z_0 \\ Ce^{-\frac{1}{2}z}\left(z\ln z - \frac{1}{\lambda}\right), & z > z_0. \end{cases} \quad (32)$$

The constant C is determined by the continuity condition

$$C = \frac{\cos(-1 + \delta\lambda^2)^{1/2}\frac{\delta}{\lambda}}{e^{-\delta/\lambda}\left(\frac{2\delta}{\lambda}\ln\frac{2\delta}{\lambda} - \frac{1}{\lambda}\right)}. \quad (33)$$

The actual wave function $\phi_{ex}(r)$ is related to $\psi(z)$ by

$$\phi_{ex}(r) = \sqrt{\frac{1}{\lambda a_0 N(\delta)}}\psi\left(\frac{2r}{\lambda a_0}\right). \quad (34)$$

The dimensionless quantity $N(\delta)$ is equal to $\int_0^\infty |\psi(z)|^2 dz$, such that $\int_{-\infty}^\infty |\phi_{ex}(r)|^2 dr = 1$. Now we substitute the trial wave function ϕ_{ex} with variational parameter δ into the expression for the quantity $G(k)$ in Eq. (23)

$$G(t,\delta) = \frac{1}{2N(\delta)}\int_{-\infty}^\infty |\psi(z)|^2 e^{it\lambda\delta z/2\delta_0} dz, \quad (35)$$

where $\delta_0 = a/a_B$ as defined above. After substituting $G(t,\delta)$ into Eqs. (23), (26), and (24), we obtain the variational ground-state energy as the function of a single variational variable δ. The ground state is then determined by minimizing the function. The vibrational excited states can be obtained by applying U_2 to states containing one or more phonons. Their energy can be obtained by calculating the expectation values of H_2 for them. For example, for states with one phonon at k, the energy is $_{ph}\langle 0|a_k H_2 a_k^\dagger|0\rangle_{ph}$.

IV. OPTICAL ABSORPTION AND EMISSION

A. Oscillator strengths

The optical absorption of conjugated polymers occurs through the creation of an exciton. This process is characterized by the oscillator strength f and the optical absorption coefficient α, both of which are related to the corresponding exciton transition-matrix element:

$$f = c_f \sum_m |P_m|^2, \quad (36)$$

$$h\nu\alpha(h\nu) = c_\alpha \sum_m |P_m|^2 \delta(E_m - E_0 - h\nu),$$

where c_f, c_α are proportional constants and $h\nu$ is the energy of the photon. The subscript m characterizes the states of the phonon. E_0 is the electronic band gap plus the ground-state energy of our Hamiltonian in Eq. (1). E_m is the energy of phonons in the final state of the optical transition. The exciton transition-matrix element for this process P_m is given by

$$P_m = \vec{\epsilon}\cdot\vec{M}_{c,v}^*\left\{\langle 0|\exp\left[\sum_{k,s}(F_k^*(0)a_{k,s}\right.\right.$$
$$\left.\left. - F_k(0)a_{k,s}^\dagger\right]|m\rangle\right\}\phi_{ex}(0)$$
$$= \vec{\epsilon}\cdot\vec{M}_{c,v}^*\exp(-g/2)$$
$$\times\langle 0|\exp\left[\sum_{k,s}F_k^*(0)a_{k,s}\right]|m\rangle\phi_{ex}(0), \quad (37)$$

where the factor g is

$$g = \sum_{k,s}|F_k(0)|^2 = n\sum_k\left(\frac{\xi}{\hbar\omega_0}\right)^2(f_k^1 - f_k^2)^2$$
$$= n\eta^2\sum_k\left(\frac{\alpha^2}{2\hbar M\omega_0^3}\right)(f_k^1 - f_k^2)^2. \quad (38)$$

Here, n is the number of even optical phonon modes. $\vec{\epsilon}$ is the unit polarization vector of the electric field, $\vec{M}_{c,v}^*$ is the dipole transition-matrix element between the valence- and conduction-band states. From the exciton transition-matrix element, we can calculate the total oscillator strength for the transition to states with a certain number of phonons. For transitions to the states with one exciton plus zero, one, and two phonons, the oscillator strengths are respectively given by

$$f^{(0)} = AL|\phi_{ex}(0)|^2\exp(-g),$$
$$f^{(1)} = f^{(0)}g, \quad (39)$$
$$f^{(2)} = f^{(0)}g^2/2.$$

The dipole transition-matrix element, the polarization vectors, and the proportional constant are all absorbed in the new constant A. L is the chain length. It is clear that the relative strength among these transitions depends on the magnitude of g. To calculate g, we need to know the parameter $\sqrt{n}\eta$, where η is the dimensionless electron-phonon coupling constant. We extract this number from the experimental emission spectra of the conjugated polymers. The transition rate, as expected, is proportional to the system size L.

Exciton radiative recombination occurs mainly after relaxation from higher phonon states to zero-phonon state. It then emits a photon and transits to the electron-hole ground state (no exciton) plus some phonons. We first assume that

the total momentum Q of the exciton in the initial state is zero. This is true for zero-temperature transition. The temperature dependence can be taken into account later. The corresponding exciton transition-matrix element for decay is similar to that of the absorption:

$$\bar{P}_m = \vec{\epsilon} \cdot \vec{M}_{c,v}^* \left\{ \langle m | \exp \left[\sum_{k,s} (F_k^*(0) a_{k,s} \right. \right.$$

$$\left. \left. - F_k(0) a_{k,s}^\dagger) \right] | 0 \rangle \right\} \phi_{ex}^*(0) \qquad (40)$$

$$= \vec{\epsilon} \cdot \vec{M}_{c,v}^* \left\{ \exp(-g/2) \right.$$

$$\times \left\langle 0 | \exp \left[\sum_{k,s} F_k^*(0) a_{k,s} \right] | m \right\rangle \right\}^* \phi_{ex}^*(0). \qquad (41)$$

The total emission rate for the various phonon final states is proportional to the square of the above matrix element integrated over the energy of the emitted photon. For an exciton with strictly zero total momentum, the emission rate to the zero, one, and two phonon states are give by

$$h^{(0)} = AL |\phi_{ex}(0)|^2 \exp(-g),$$

$$h^{(1)} = AL \exp(-g) |\phi_{ex}(0)|^2 n |F_0|^2, \qquad (42)$$

$$h^{(2)} = AL \exp(-g) |\phi_{ex}(0)|^2 \frac{n^2}{2} \sum_k |F_k F_{-k}|^2.$$

Because of momentum conservation, only the phonon with zero momentum can be emitted in the one-phonon process, and the two phonons must be of opposite momenta k and $-k$ in the two-phonon process. To be selfconsistent, the emission rate should remain finite as the chain length L goes to infinity. As shown in Eqs. (9) and (15), the quantity F_k scales as $L^{-1/2}$. The emission rates for the one and two phonon processes, indeed, do not scale with L. However, the zero-phonon emission rate $h^{(0)}$ is proportional to L. This problem can be fixed only when we consider the case of finite temperature.

At finite temperature, the exciton total momentum Q is allowed to thermally fluctuate and become nonzero. However, the final state, electron-hole ground state with no phonon, has a total momentum equal to zero. From momentum conservation, the rate is nonzero only for initial states with zero total momentum, which, as the length L of the polymer chain becomes large, occupies a phase space scaling with the inverse of L. The transition rate is the product of $h^{(0)}$ and the probability that the exciton momentum $Q = 0$. Since the two factors have inverse scaling with respect to L, the physical rate stays finite as L goes to infinity. We assume that the probability distribution is determined by a Boltzman distribution

$$P(Q) = \frac{1}{L} \sqrt{\frac{2\beta \hbar^2 \pi}{m^*}} \exp \left(-\beta \frac{\hbar^2 Q^2}{2m^*} \right). \qquad (43)$$

By the periodic boundary condition, Q takes the discrete values $2\pi m/L$, with m being an integer. The normalization of the probability distribution is determined by

$$\sum_Q P(Q) = \frac{L}{2\pi} \int_{-\infty}^\infty P(Q) dQ = 1. \qquad (44)$$

Because of the momentum conservation, only excitons with $Q = 0$ can decay radiatively. Thus the temperature-dependent zero-phonon emission rate $\Gamma_0(T)$ is given by

$$\Gamma_0(T) \simeq h^{(0)} \sum_Q P(Q) \delta_{Q,0} = h^{(0)} \int_{-\infty}^\infty P(Q) \delta(Q) dQ$$

$$= h^{(0)} P(0) = A |\phi_{ex}|^2 e^{-g} \sqrt{\frac{2\beta \hbar^2 \pi}{m^*}}. \qquad (45)$$

Now the zero-phonon emission rate is now finite as L becomes infinity. The above formula Eq. (45), however, implies strong temperature dependence of the zero-phonon emission rate, which is not observed experimentally. The reason is that the sharp Dirac δ function $\delta(Q)$ above should be, in reality, replaced by a distribution function with finite width ΔK. The strict momentum selection rule is smeared by defects or environmental inhomogeneity, which break the discrete translational invariance. So, we replace the Dirac δ function in Eq. (45) by a Lorentzian distribution $\mathcal{L}(Q; \Delta K) = (\pi \Delta K)^{-1} [1 + (Q/\Delta K)^2]^{-1}$ with width ΔK. The zero-phonon emission rate becomes

$$\Gamma_0(T) \simeq h^{(0)} \int_{-\infty}^\infty P(Q) \mathcal{L}(Q; \Delta K) dQ$$

$$= h^{(0)} \frac{2\pi}{L} \frac{1}{\pi \Delta K} r(T; \Delta K)$$

$$= A |\phi_{ex}(0)|^2 e^{-g} \frac{2}{\Delta K} r(T; \Delta K). \qquad (46)$$

The dimensionless parameter $r(T; \Delta K)$ is equal to

$$r(T; \Delta K) = \frac{L}{2\pi} \int_{-\infty}^\infty P(Q) \frac{1}{1 + \left(\frac{Q}{\Delta K} \right)^2} dQ$$

$$= \frac{1}{\sqrt{\pi}} \int_0^\infty e^{-\epsilon} \frac{1}{\sqrt{\epsilon}} \frac{1}{1 + \frac{\epsilon}{\Delta E \beta}} d\epsilon. \qquad (47)$$

Here, ΔE is the corresponding energy range and we assume that it equals $(\Delta K)^2/2M$. r is basically the fraction of the thermal probability distribution that is within the range of ΔK. When the temperature goes to zero, r approaches one accordingly.

While such replacement has significant effect on the temperature dependence of the zero-phonon emission rate, it does not affect other phonon bands. For one or more phonon emission, there is always a continuum of available final states with arbitrary phonon momentum. In addition, the transition rate $h^{(1)}$ is not sensitive to the exciton momentum Q. Thus, the one-phonon emission rate $\Gamma^{(1)}(T)$ at finite temperature can be written as

$$\Gamma^{(1)}(T) \simeq h^{(1)} \sum_{K,Q} P(Q) \delta_{K,Q} = h^{(1)} \sum_Q P(Q)$$

$$\times \int_{-\infty}^{\infty} \delta(K-Q) dK = h^{(1)}. \qquad (48)$$

Here, Q is the momentum of the exciton (initial state) and K is the momentum of the emitted phonon (final state). The δ function above indicates that the momentum conservation is strictly enforced. Clearly, it does not matter whether we use a δ function or a distribution with finite width. The formula also shows that the one-phonon rate is insensitive to T and ΔK. The case for two-phonon emission rate is similar, i.e.,

$$\Gamma^{(2)}(T) \simeq h^{(2)}. \qquad (49)$$

Our model thus predicts a mild temperature dependence for zero-phonon emission rate while the multiple phonon emission rates are temperature independent.

B. Line shapes

Now we turn to the line shapes of the absorption and emission spectra. So far, we consider only a single chain, and the line shape of the spectra is give by Eq. (36). However in real sample the inhomogeniety broadening seems to dominate over the theoretical line shapes. We observe that the experimental linewidth is 70 meV at 20 K, which is much larger than the theoretical linewidth, i.e. the thermal energy $k_B T$. This difference shows that the experimental broadening is of disorder origin, instead of intrinsic origins like thermal fluctuation and electronic bandwidth. Consequently, in order to make a reliable prediction on the gain profile, we choose not to use the theoretical line shapes. Instead, we attach Gaussian distributions with adjustable width to the phonon bands with the corresponding oscillator strength. In Sec. IV C, a fitting of our prediction with the observed emission spectra will be described, which shows almost perfect match and confirms our assumption of Gaussian distributions here.

The absorption rate $\alpha_c(\nu)$ as a function of the photon frequency can be written as

$$\alpha_c(\nu) = \alpha_{c0}(\nu) + \alpha_{c1}(\nu) + \alpha_{c2}(\nu), \qquad (50)$$

with

$$\alpha_{ci}(\nu) = f^{(i)} \mathcal{F}_i(\nu), \quad \mathcal{F}_i(\nu) = \frac{1}{\sqrt{\pi}\sigma_i^a} \exp\left[-\left(\frac{\nu - \nu_i^a}{\sigma_i^a}\right)^2\right]. \qquad (51)$$

The subscript "c" denotes chain. $f^{(i)}$ is the absorption oscillator strength for the ith sideband obtained in Eq. (39), and $\mathcal{F}_i(\nu)$ the Gaussian distribution centered at the peak frequencies ν_i^a of the sidebands in the absorption spectrum. σ^a is the line broadening for the absorption spectrum. It is convenient to factor out the physical dimension and define a dimensionless line-shape function $\bar{\alpha}(\nu)$:

$$\alpha_c(\nu) = \frac{LA|\phi_{ex}(0)|^2 e^{-g}}{\sqrt{\pi}\sigma_1^a} \bar{\alpha}(\nu), \qquad (52)$$

where $\bar{\alpha}(\nu)$ is given by

$$\bar{\alpha}(\nu) = \sqrt{\pi}\sigma_1^a [\mathcal{F}_0(\nu) + g\mathcal{F}_1(\nu) + \tfrac{1}{2}g^2 \mathcal{F}_2(\nu)]. \qquad (53)$$

Now, we consider the absorption coefficient α. For a real sample made out of a large number of chains, the absorption coefficient $\alpha(\nu)$ is proportional to the single-chain absorption rate $\alpha_c(\nu)$ times the volumn density of chains, which is determined by chain packing geometry. We can combine the chain density, the factor $LA|\phi_{ex}(0)|^2 e^{-g}$ in Eq. (52) and the proportional constant into a common dimensionful constant B for all the phonon sidebands and write

$$\alpha(\nu) = B\bar{\alpha}(\nu). \qquad (54)$$

B has the same unit of cm^{-1} as the absorption coefficient α.

Similarly, the recombination rate $\gamma_c(\nu)$ for an exciton in a single chain can be written as

$$\gamma_c(\nu) = \gamma_{c0}(\nu) + \gamma_{c1}(\nu) + \gamma_{c2}(\nu), \qquad (55)$$

with

$$\gamma_{ci}(\nu) = \Gamma^{(i)} \mathcal{G}_i(\nu), \quad \mathcal{G}_i(\nu) = \frac{1}{\sqrt{\pi}\sigma_i^e} \exp\left[-\left(\frac{\nu - \nu_i^e}{\sigma_i^e}\right)^2\right]. \qquad (56)$$

$\mathcal{G}_i(\nu)$ is the Gaussian distribution centered at the peak of the phonon sideband in the emission spectrum. Plugging in the oscillator strength $\Gamma^{(i)}$, we have

$$\gamma_c(\nu) = \frac{Aa|\phi_{ex}|^2 e^{-g}}{\sqrt{\pi}\sigma_1^e} \bar{\gamma}(\nu). \qquad (57)$$

The dimensionless function $\bar{\gamma}(\nu)$ is

$$\bar{\gamma}(\nu) = \sqrt{\pi}\sigma_1^e \left[\frac{2\pi}{\Delta Ka} r(T;\Delta K) \mathcal{G}_0(\nu) + \frac{L}{a} n |F_0|^2 \mathcal{G}_1(\nu) \right.$$

$$\left. + \frac{L}{a} \frac{n^2}{2} \sum_k |F_k F_{-k}|^2 \mathcal{G}_2(\nu) \right]. \qquad (58)$$

When there are N_{ex} excitons in the chain, the photon emission rate becomes

$$\gamma_c(\nu) N_{ex} = LA|\phi_{ex}|^2 e^{-g}(n_{ex}a)\bar{\gamma}(\nu), \qquad (59)$$

where $n_{ex} \equiv N_{ex}/L$ is the chain exciton density. $n_{ex}a$ is the number of excitons per unit cell. For the same reason as in absorption, the photon emission coefficient $\gamma(\nu, n_{ex})$ for a real sample can be written as

$$\gamma(\nu, n_{ex}) = B n_{ex} a \bar{\gamma}(\nu). \qquad (60)$$

The factor B here is the same as the one in Eq. (54) since the absorption and emission processes do not differ in chain packing geometry and dipole matrix element. The optical spectra are thus determined up to a common factor B, which can only be fixed by comparing with the experiment. Combining the absorption spectrum and the stimulated emission spectrum, we can obtain the gain coefficient of the sample. This will be discussed in Sec. V.
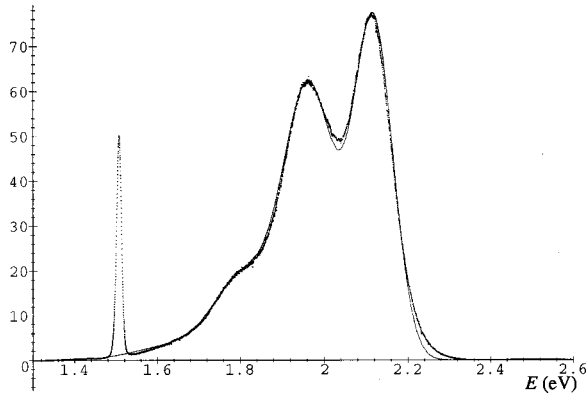
FIG. 1. The observed emission spectrum of Pd0PV film at 300 K. The solid line indicates the theoretical fitting using three Gaussian distributions corresponding to zero-, one- and two-phonon emission.

C. Comparison with experiments and predictions

We try to fit the recently observed[14] emission spectra of the various conjugated polymers by three equally spaced Gaussian distributions, as suggested in Eq. (55). Figure 1 is the fitting for poly(dioctyloxy phenylene vinylene) (Pd0PV) film at 300 K. As clearly shown in the figure, the data perfectly match the sum of three Gaussian distributions. This is also true for Pd0PV film at 10 K, Pd0PV solution at 300 K and poly(2-methoxy,5-(2′ethyl)-hexyloxy-phenylene-vinylene) (MEH-PPV) solution at 300 K. From the fitting, we can determine σ_i^e, ν_i^e and $\Gamma^{(i)}$. For simplicity, we assume that the absorption and emission roughly share the same broadening, i.e., $\sigma_i^a = \sigma_i^e$. From the ratio of $\Gamma^{(2)}$ and $\Gamma^{(1)}$, we can deduce the product of η, the effective electron-phonon coupling constant, and $\sqrt{n}$. They always appear together in the calculation. The wave function ϕ_{ex} and associated variables such as $f_k^{1,2}$ are evaluated using the variational method described in Sec. III. We choose $m_e = 0.117m_0$ and $m_h = 0.0658m_0$, here m_0 is the free-electron mass.[15] The dielectric constant ϵ is set to 3. The wave number of the phonon is deduced from the spacing between the emission phonon sidebands, which corresponds to 1454 cm^{-1}. With $\sqrt{n}\,\eta$, we can calculate the factor g in Eq. (38), which determines the oscillator strength of absorption. Thus we obtain a prediction for the absorption spectra. This prediction will be used in the next section to discuss the optical gain. Direct comparison of the predicted absorption spectrum with experiment is so far difficult, because the phonon structures are washed away by the chain length distribution and other

TABLE I. The ratio among the experimental emission phonon sidebands Γ_i, the fitted electron-phonon couling constant $\sqrt{n}\,\eta$, the corresponding phonon displacement factor g, and the fitted momentum smearing ΔK are shown for various samples and conditions.

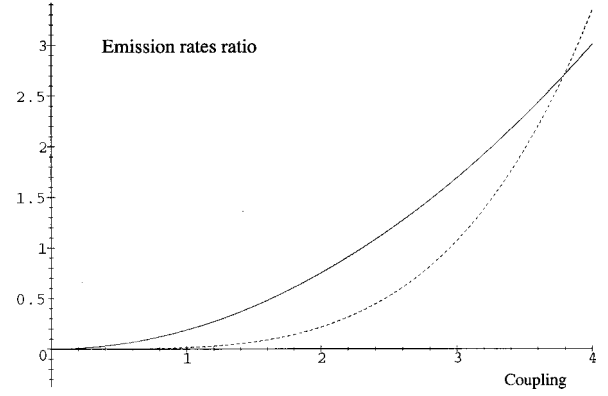| Material	Γ_0/Γ_1	Γ_1/Γ_2	$\sqrt{n}\,\eta$	g	$a\Delta K$
Pd0PV film 300 K	0.91	3.33	2.1	0.94	0.17
Pd0PV film 10 K	1.14	3.23	2.1	0.94	0.19
Pd0PV solution 300 K	1.37	3.33	2.1	0.94	0.07
MEH-PPV solution 300 K	1.27	3.12	2.2	1.03	0.08

FIG. 2. The ratios of the one phonon (solid line) and two phonon emission rates (dashed line) to the zero phonon emission rate as a function of the effective coupling parameter $\sqrt{n}\,\eta$.

broadening mechanisms. On the other hand, the ratio between $\Gamma^{(1)}$ and $\Gamma^{(0)}$ determines the parameter ΔK. The fitting for the 300 and 10 K Pd0PV film data gives ΔK equal to $0.17/a$ and $0.19/a$, respectively. The fact that they are so close confirms our explanation of the temparature dependence. The results of $\sqrt{n}\,\eta$ and ΔK for four kinds of conjugated polymers are shown in Table I.

The effective electron-phonon coupling constant η may be different for other conjugated polymers. In Figs. 2 and 3 we plot the strength of the higher phonon sidebands relative to the zero-phonon band for the absorption and the emission spectra as functions of $\sqrt{n}\,\eta$. For larger $\sqrt{n}\,\eta$, the phonon modes are more displaced in the excited state with respect to the ground state. The spectra are consequently more dominated by the higher phonon bands.

V. OPTICAL GAIN

Excitons are created through either optical excitation or electron-hole current injection. In addition to the spontaneous decay discussed in the previous section, excitons can also decay radiatively through stimulated emission. Therefore, in the presence of excitons, an electromangetic wave propagating in the polymer sample may experience net gain and be amplified. Gain is achieved when stimulated emission
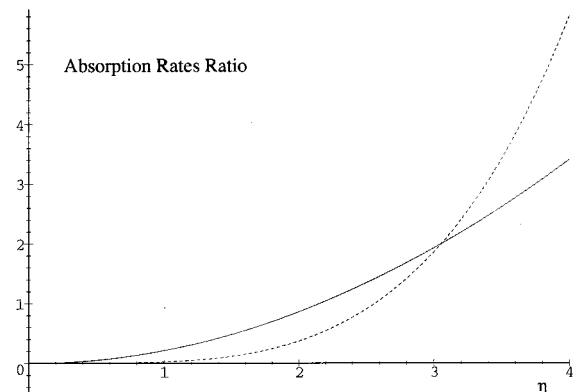

FIG. 3. The ratios of the one-phonon (solid line) and two-phonon absorption rates (dashed line) to the zero-phonon absorption rate as a function of the effective coupling parameter $\sqrt{n}\,\eta$.
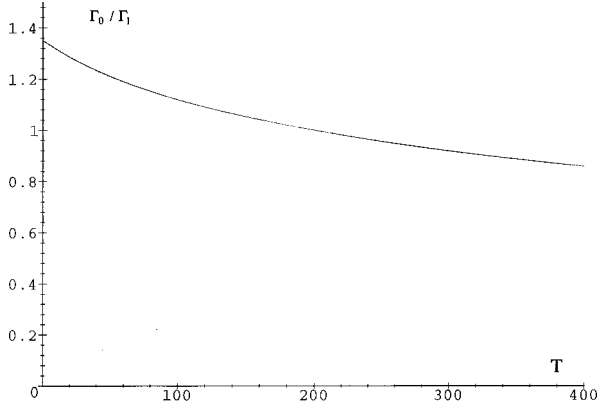
FIG. 4. The ratio of Γ_0 over Γ_1 as a function of temparature T.

has a higher rate than absorption. It is more likely to occur in the emission spectral region where overlap with the absorption spectrum is minimal. Our calculation on the relative strength of the phonon sidebands shows that, due to vibrational relaxation, there is a significant redshift of the emission spectrum relative to the absorption. Such shift reduces the spectral overlap and favors gain. Below, we first study the gain coefficient for arbitrary frequency and exciton density, then compare our prediction with the experiment.

The gain coefficient $g(\nu)$ is the difference between the emission coefficient and the absorption coefficient

$$g(\nu) = \gamma(\nu, n_{ex}) - \alpha(\nu) = B\bar{g}(\nu), \qquad (61)$$

with

$$\bar{g}(\nu) = (n_{ex}a)\bar{\gamma}(\nu) - \bar{\alpha}(\nu). \qquad (62)$$

It depends only on the intrinsic properties of the polymer chain, i.e., $\gamma(\nu)$ and $\alpha(\nu)$, as well as the number of exciton N_{ex} in the chain. With the dimensionful constant B pulled out, the function $\bar{g}(\nu)$ is dimensionless. For a given frequncy ν, net gain is achieved when $g(\nu) > 0$. In other words, the threshold exciton density n_{ex}^T is given by
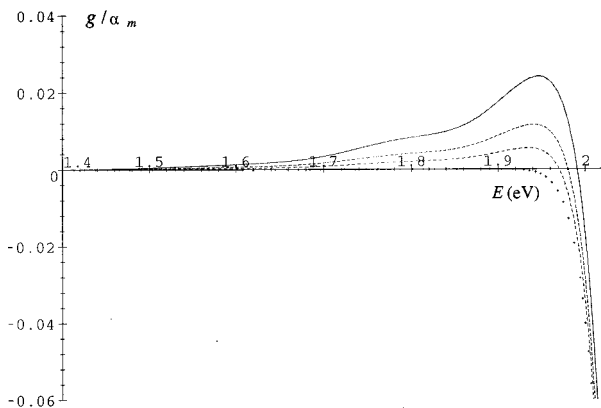

FIG. 5. Optical gain coefficients $g(\nu)$ of Pd0PV film at 300 K with exciton densities n_{ex} equal to 0.004 (solid line), 0.002, 0.001 (dashed line) and 10^{-5} (crossed line), normalized so that the peak absorption rate α_m is equal to 1.
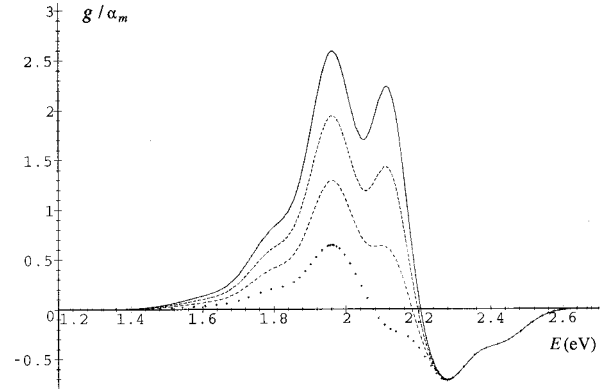

FIG. 6. Optical gain coefficients $g(\nu)$ of Pd0PV film at 300 K with exciton densities n_{ex} equal to 0.4 (solid line), 0.3, 0.2 (dashed line), and 0.1 (crossed line), normalized so that the peak absorption rate α_m is equal to 1.

$$n_{ex}^T a = \frac{\bar{\gamma}(\nu)}{\bar{\alpha}(\nu)}. \qquad (63)$$

In the emission spectral region where overlap with the absorption spectrum is small, we have

$$\bar{\gamma} \gg \bar{\alpha}, \quad n_{ex}^T a \ll 1. \qquad (64)$$

$n_{ex}a$ is the fraction of the valence-band electrons that are excited to the conduction-band and form excitons. Therefore, in this case gain will occur even though only a small fraction of electrons in the valence band are excited (see Fig. 4).

The optical gain depends on the constant B. Though we cannot calculate B, it can be inferred from the experimental data. Especially the maximum of the absorption coefficient α_m can be measured directly. Let us discuss Pd0PV film at room temparature as an example. According to our model, in this case the maximum of the absorption occurs at the center of the zero-phonon band ν_0^e, i.e., $\alpha_m = \alpha(\nu_0^a) = B$. Hence the calculable dimensionless function $\bar{g}$ is equal to the gain coefficient $g(\nu; n_{ex})$ divided by α_m. In Figs. 5, 6, and 7, we plot the dimensionless function $g(\nu)/\alpha_m$ for various exciton densities $n_{ex}a$. As shown in Fig. 5, gain indeed occurs for the spectral region around the one-phonon emission band
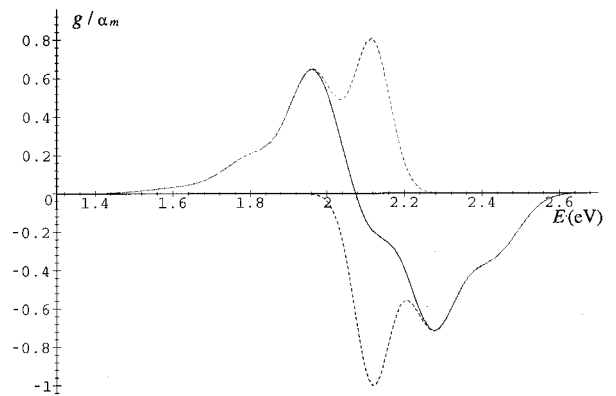

FIG. 7. The gain coefficient $g(\nu)$, emission rate and absorption rate (dashed lines) of Pd0PV film at 300 K with exciton densities n_{ex} equal to 0.1, all normalized so that the peak absorption rate α_m is equal to 1.
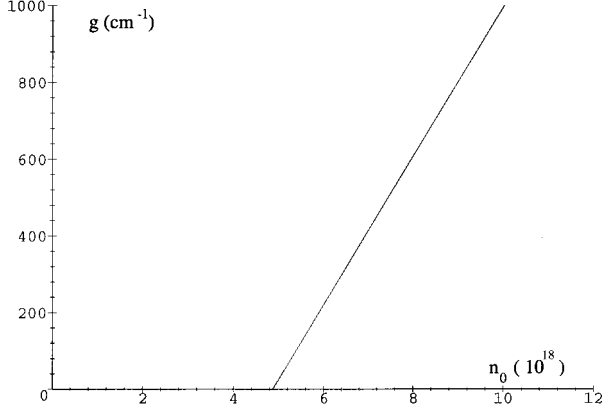
FIG. 8. The gain coefficient as a function of the exciton volumne density n_0 at the maximal gain frequency of ν_1^e.

TABLE II. Based on the experimental threshold exciton density n_0, our predicted resonator loss α_r(theo) is compared with the experimental estimate α_r(exp).

	Ref. 4	Ref. 17	Ref. 5
n_0^T(exp)/cm^{-3}	1.4×10^{20}	7.4×10^{17}	$\sim 10^{17}$
α_r(theo)/cm^{-1}	2.7×10^4	146	~ 20
α_r(exp)/cm^{-1}	1.8×10^4	$10 \sim 100$	$10 \sim 100$

once the exciton density is above 10^{-4} per unit cell. The maximum absorption α_m for PPV film has been estimated[14] to be about 2.3×10^5 cm^{-1}. Since $\alpha_m = B$, we have $B = 2.3 \times 10^5$ cm^{-1}. We denote this value as B_0 for reference.

We concentrate now on the gain profile near the maximal gain frequency ν_1^e. According to our model calculation, $\bar{\gamma}(\nu_1^e) = 6.4$ and $\bar{\alpha}(\nu_1^e) = 0.004$. For comparison with experiments, it is convenient to use the volume density of exciton, n_0, instead of the chain density n_{ex}. n_0 is related to n_{ex} by $n_0 = n_{ex}a/v_0$, where v_0 is the primitive cell volume. The density of the unsubstituted PPV unit cell has been estimated[16] to be 7.5×10^{21} cm^{-3}, corresponding to a primitive cell volume v_0 of 1.3×10^{-22} cm^3. In Fig. 8, we plot the gain coefficient as a function of the exciton volume density n_0 at ν_1^e. The onset of gain at the peak of the one-phonon emission band ν_1^e is at $n_{ex}a = 6.3 \times 10^{-4}$. The corresponding threshold exciton volume density n_0^T for gain is therefore 4.8×10^{18} cm^{-3}.

So far, we considered only the optical gain due to the active medium of conjugated polymers. In order to make a practical estimate on the exciton density required for lasing action in a resonator, we also need to know the resonator loss coefficient $\alpha_r(\nu)$, which arises from the loss mechanisms such as free-carrier absorption, scattering from optical inhomogeneities, and imperfect mirror reflection. $\alpha_r(\nu)$ is, of course, sensitive to material and mirror quality and is expected to vary from case to case. The actual threshold of lasing is determined by the competition between the active medium gain $g(\nu)$ considered above and the resonator loss $\alpha_r(\nu)$. Lasing occurs only when the former is larger than the latter.

If this actual threshold chain density $n_{ex}a$ is much larger than the ratio between $\bar{\gamma}$ and $\bar{\alpha}$, the formula can be simplified significantly. For frequencies close to ν_1^e, $\bar{\gamma} \sim 10^3 \bar{\alpha}$. It is hence a good approximation to ignore α in Eq. (61) if $n_{ex}a \gg 10^{-3}$, i.e.,

$$g(\nu) \simeq B_0 n_{ex}a \bar{\gamma}(\nu) = B_0 v_0 n_0 \bar{\gamma}. \quad (65)$$

With this approximation, our prediction for the gain coefficient can be easily generalized to polymers of different struc-

tures. For PPV polymer samples with other packing geometry, the primitive cell volume v and the constant B are different from v_0 and B_0. However, B is proportional to the density of chains. Therefore, the product of B and the primitive cell volume is a constant, i.e., $Bv = B_0 v_0$, assuming that one chain contains roughly identical numbers of primitive cells. The gain coefficient for a sample with an arbitrary v is then

$$g = B v n_0 \bar{\gamma} = B_0 v_0 n_0 \bar{\gamma} = 3.1 \times 10^{-17} \bar{\gamma} n_0 \text{ cm}^2, \quad (66)$$

where $n_0 = n_{ex}a/v$ is the exciton volume density for this sample. Note that this formula is independent of v. It thus applies to samples with arbitrary packing geometry and density, including even polymer blends for which the active polymer(PPV) is dispersed in an inert matrix. The equation above gives a relation between the resonator loss α_r and the actual threshold exciton volume density n_0^T

$$\alpha_r = 3.1 \times 10^{-17} \bar{\gamma} n_0^T \text{ cm}^2. \quad (67)$$

For Pd0PV at room temperature, $\bar{\gamma} = 6.4$ at the peak gain. Thus,

$$\alpha_r = 1.98 \times 10^{-16} n_0^T \text{ cm}^2. \quad (68)$$

This treatment can be easily generalized to other PPV derivative that are similar. The above relation holds for room-temparature Pd0PV samples of any form.

To check the relation Eq. (68), we obtain the corresponding resonator loss coefficient α_r(theo) from the threshold density n_0^T estimated by the various experimental groups. α_r(theo) is then compared with the experimental values α_r(exp). The results are shown in Table II for the experimental data by Tessler et al. (Ref. 4), Frolov et al. (Ref. 17) and Wegmann et al. (Ref. 5). The difference between the theoretical predictions and the experiment data on the resonator loss coefficient are within 50%. No adjustable parameter is introduced in this comparison. This check confirms the reliability of the relation Eq. (67). The values of n_0^T(exp) for Refs. 4 and 17 are estimated from the excitation laser pulse energy, focus area, and the ratio between exciton lifetime and the pulse duration. For Ref. 5, it is given by the author. The condition $n_{ex}a \gtrsim 10^{-3}$ is satisfied in all cases. We estimate the values of α_r(exp) by separating it into two parts: $\alpha_r = \alpha_s + \alpha_m$, where the former is due to inhomogeneity scattering and the latter imperfect mirror reflection. α_m is equal to $(\ln R)/2d$, where R is the mirror reflectance and d is the resonator length. α_s is assumed to take the usual magnitute of $10 \sim 100$ cm^{-1}.[18] In Ref. 4, α_m is estimated to be 1.8×10^4 cm^{-1} with $d = 100$ nm and $R = 0.7$. The scattering

loss is much smaller and can be neglected in this case. For the case of Ref. 17, α_m is estimated to be 0.18 cm^{-1} with $d=4.5$ cm and $R=0.2$. It is much smaller than the scattering loss and can be ignored. There is no mirror used in Ref. 5 and the surface reflectance in unknown; we assume that the loss is also dominated by the scattering just like Ref. 17.

VI. DISCUSSION

We present in this article a model to study the interaction of the excitons and the optical phonons in conjugated polymers. In our model, there is only one adjustable parameter η, the strength of the electron-phonon coupling. The value of η is different for different kinds of polymers since the lattice dynamic equation depends on the backbone structure as well as the side groups of the polymers. η is a combination of the phonon polarization vectors $\epsilon_s^i(k)$, and is, in principle, calculable. η should be of order one, because the polarization vectors are all properly normalized. However, it is too complicated to calculate η this way. For PPV, each unit cell contains eight carbon atoms. There are a total of sixteen degrees of freedom even if we consider only the motion of the atoms within the benzene plane. The normal modes will include fourteen optical phonon branches plus two acoustic branches. The lattice dynamic equation is thus quite involved. Instead of calculating it microscopically from the lattice structure, we determine the value of η by fitting the experimental data of the relative oscillator strength of the photoluminescence phonon sidebands. However, it turns out that the strength of the zero-phonon band has an observable temperature dependence. In order to fit the temperature dependence of the zero phonon emission oscillator strength, we introduce another parameter ΔK, which is the smearing of the momentum selection rule. The optical transition is allowed as long as the difference between the initial and final crystal momenta is within ΔK. The microscopic origin of the smearing includes, for example, lattice distortion, which breaks the discrete translational symmetry, and the emission of acoustic phonons in the process. As discussed in section IV, the oscillator strength of the one and two phonon sidebands in the luminescence spectrum are both independent of ΔK, while the strength for the zero-phonon band depends on ΔK mildly. The electron-phonon coupling constant η is thus determined by the ratio between the one phonon and the two phonon luminescence sidebands, since this ratio is independent of the extra parameter ΔK. In other words, even though the value of ΔK may vary slightly from sample to sample, this uncertainty has no effect on the determination of the intrinsic adjustable parameter η. In Sec. IV, η for two PPV derivatives (MEH-PPV and PdOPV), both in film and solution, are determined. Their values differ by at most 7%. We, therefore, consider this value quite reliable. By fitting the experimental ratio between the strengths of the one- and zero-phonon sidebands, we determine the momentum smearing parameter ΔK. For our samples, it is about $0.17/a$, which is about 6% of the size of the first Brillouin zone. This is also quite reasonable. One of our main results is that once the electron-phonon coupling constant η is determined by fitting the luminesence spectrum, we can use it to predict the

relative phonon sidebands of the absorption spectrum. For the absorption spectrum, none of the sidebands depend on the momentum smearing ΔK. They depend only on one single parameter η through the factor $g(\eta)$, as seen in Fig. 3. As shown in Sec. IV, the one-phonon sideband is as important as the zero-phonon band, if the material quality can be improved to suppress the imhomogeniety broadening. The large weighting of the one-phonon band reduces the overlap between the absorption and the emission spectra and gives rise to gain in the emission spectral region. In Sec. V we use the calculated absorption spectrum together with the experimental emission spectrum to make quantitative predictions on the gain spectrum of the polymer sample.

The existence of a genuine Stokes shift has been addressed by some site-selective photoluminescence (PL) experiments recently.[9,10] In those experiments, the excitation is chosen to be deeply inside the low energy tail of the absorption spectrum to ensure that only long chains are excited, so that no subsequent exciton migration to other chains occurs before emission. The work by Heun *et al.* shows that for PPV films the zero-phonon band of the PL is quite close to the excitation energy,[10] whereas Samuel *et al.* found that the energy of the zero-phonon band is unresolvable but the one-phonon band is about one optical phonon energy below the excitation energy. Those authors, thus, concluded that the site-selective absorption is dominated by the zero-phonon band in the absorption spectrum, implying there is no excited state relaxation among the vibrational levels, i.e., a vanishing genuine Stokes shift. However, such interpretation is somewhat over simplified, because in the site-selective experiments the polymers are most likely to be excited to the zero-phonon states even if the oscillator strength of the higher phonon band is larger than the zero-phonon band. The reason is that the excitation is in the lower energy tail of the DOS, where the population of chains is supposed to increase exponentially with their electronic transition energy. Therefore, for a given excitation energy, the population of the chains whose zero-phonon band matches the excitation is much larger than the population of the chains whose higher phonon bands matches the excitation. This is simply because the electronic energy of the former is one or more optical phonon energy above the latter. For PPV film, the DOS is estimated to be a Gaussian distribution with variance about 46 meV.[19] Since the optical phonon energy is about 0.2 eV, for a given excitation energy the population of the chains excited to the one-phonon states is about only one percent of the population of chains excited to the zero-phonon states. Therefore, unless the oscillator strength of the one-phonon band is one hundred times larger than the zero-phonon band, the site-selective absorption is always dominated by the zero-phonon band. Such dramatic contrast in the oscillator strengths is, of course, very unlikely. In other words, the interpretation of such experiments is complicated by the sharp DOS decay in the energy tail, and the lack of excited state energy relaxation cannot be used to rule out the possibility of dominant higher-phonon oscillator strength for one single chain.

Even though conjugated polymers behave like semiconductors in many aspects, the gain mechanism is quite different from the conventional semiconductor lasers based on III-V compounds. In compound semiconductors there is ba-

sically no Stokes shift due to excited state lattice relaxation. Gain is achieved only when the pumping is so strong that the initial states are depleted and the final states are filled, i.e., when the quasi-Fermi level for the electrons is pushed up into the conduction band and the quasi-Fermi level for the hole is pulled down into the valence band. Under such pumping level, the absorption and emission spectra are displaced with respect each other to allow a net gain. In other words, the intensity of the pumping beam must be in the nonlinear regime where the absorption starts to saturate. In conjugated polymers, no such depletion is required because the vibrational relaxation in the excited state automatically provides the redshift of emission respect to absorption, even when the pumping intensity is still low in the linear regime, where the absorption remains basically the same as the ground state. This situation is actually similar to the case of excimer laser, for which population inversion is automatically realized because excimers form only in the excited state. The only difference is that for excimers the Stokes shift is due to the intermolecular distance relaxation, while for conjugated polymers it is due to the intrachain lattice relaxation involving extended phonon modes.

In Sec. V, we check our theoretical prediction on the relation between the lasing threshold and the resonator loss with experiment data. Our prediction of the resonator mirror loss agrees with the experiment within 50% (Ref. 4). In the case of the scattering loss, accurate comparison with the experiment is impossible because the optical characteristics of the polymer films used in the experiment are not specified. Nonetheless the predictions are all in the right order of magnitude (Refs. 17 and 5). We also estimate the minimum threshold exciton density for lasing to be realized in PPV samples. In the experiment of the Cambridge group,[4] one end of the 100-nm resonator containing the polymer film is a distributed Bragg reflector with reflectance of about 70%. The corresponding loss is about 1.8×10^5 cm^{-1}. The total resonator loss is expected to be dominated by the mirrors. We found that to overcome a resonator loss of the order of 10^4 cm^{-1}, a volume exciton density of the order of 10^{20} cm^{-3} is required. This is much larger than the typical lasing threshold of about 10^{18} cm^{-3} for conventional compound semiconductor laser. However, if the DBR is replaced by a high-reflectance mirror, the resonator loss can be reduced to the residual loss from mechanisms like light scattering by optical inhomogeneity and defect absorption. The loss is usually of the order of only $10-100$ cm^{-1}. The volume exciton density required to overcome this loss is predicted to be only of the order of 10^{17} cm^{-3}. This threshold density is then smaller than that of the conventional semiconductor lasers. The corresponding exciton number per PPV monomer $n_{ex}a$, is as low as 10^{-4}. This is the range shown in Fig. 5. So in principle gain can be realized in high-reflectance resonators when there is only one exciton per ten thousand PPV monomers. Unfortuantely, when a polymer sample is sandwiched between two mirrors of high reflectance, it can no longer be optically excited from outside easily. The question now is whether it is possible to generate excitons to the density of the order of 10^{17} cm^{-3} through electric current injection. This corresponds to the level of excitations required for electrically pumped polymer laser. The obstacle to electric pumping of conjugated polymer laser

is twofold. One is the difficulties of carrier injection. Another is related to the fact that, even if current can be easily injected, the electrons and holes form both singlet and triplet excitons, with a rough ratio of 1:3 based on spin statistics. In most cases, the triplet exciton energy is actually lower than the singlet. The singlet ratio is thus even lower than 25%. Only singlet excitons will undergo optical transitions. The corresponding total exciton density required for electric pumping polymer laser with residual loss of 10 -100 cm^{-1} is therefore around 10^{18} cm^{-3}, comparable to the typical density for compound semiconductor lasers. Still, as discussed above, the corresponding total number of exciton per PPV monomer is only less than 10^{-3}. There is no fundamental reason preventing the realization of such exciton density, if the injection problem can be solved.

Photoinduced absorption due to interchain excited state, which spectrally overlaps with the stimulated emission, has been reported to be an important factor to diminish the gain for some polymer samples. It has been argued that interchain species, identified as excimers or polaron pairs, have a dominating quantum yield.[20,21] Such claims are, however, contradicted by other works on the absolute PL quantum efficiency,[22] and some controversies remain. Even though interchains species do seem to appear in high-quantum yield for some polymers such as CN-PPV,[23] their polulation can be controlled by the side groups. For example, large and bulky side groups will presumably isolate the polymer backbones from each other and prevent the formation of interchain species. In this paper, we do not attempt to include the effect of such species.

The wavelength at which the gain coefficient is maximal depends slightly on the side groups of PPV. In general, the emission spectrum of unsubstituted PPV is blueshifted with respect to other soluble derivatives. The possible reason is that the former is polymerized only after coating on the substrate, while the latter can be directly spin coated in the polymer form. The effective conjugation length of unsubstituted PPV film is therefore expected to be smaller than films made of other derivatives. This explains its higher band gap and emission spectrum. Our theoretical calculations do not assume any particular value of the band gap. Therefore, the predictions on the gain coefficient around the one-phonon emission peak does not depend on where it actually is. For example, the peak is at 2.35 eV (547 nm) for PPV, and 1.95 eV (631 nm) for MEH-PPV.

VII. CONCLUSION

Starting from a model Hamiltonian for the exciton-phonon coupling, we study the absorption and luminescnece spectra including the phonon side bands. The electron-phonon coupling constant is the only fitting parameter, determined by fitting the experimental ratio between the one- and two-phonon sidebands in the photoluminescence spectrum. We then calculate the absorption spectrum and predict that the one phonon band is as important as the zero-phonon band. This is contrary to the case of luminescence, which is dominated by the zero-phonon band for the samples we considered. The gain coefficient is calculated based on the results. We derive a general relation between the resonator loss

and the volume exciton density required for lasing threshold, applicable to PPV samples with arbitrary packing geometry and density. Our result is in good agreement with the experiments for both high- and low-loss resonators. For low-loss resonator with loss of $10-100$ cm^{-1}, the threshold singlet exciton density required for lasing action is of the order of 10^{17} cm^{-3}. This is, to our knowledge, the first theoretical work that makes quantitative predictions on the gain spectrum of such systems. The implication on the feasibility of polymer laser based on PPV is discussed.

*Electronic address: meng@cc.nctu.edu.tw

†Electronic address: chchang@phy03.phy.ntnu.edu.tw

[1] For review, see S. Greenham and R. Friend, in *Solid State Physcs*, edited by H. Ehrenreich and F. Spaepen (Academic Press, Boston, 1995).

[2] J. Burroughes, D. Bradley, A. Brown, R. Marks, K. Mackay, R. Friend, P. Burns, and A. Holmes, Nature (London) **347**, 539 (1990).

[3] D. Moses, Appl. Phys. Lett. **60**, 3215 (1992).

[4] N. Tessler, G. Denton, and R. Friend, Nature (London) **382**, 539 (1996).

[5] G. Wegmann, H. Giessen, A. Greiner, and R. Mahrt, Phys. Rev. B **57**, R4218 (1998).

[6] M. McGehee, R. Gupta, S. Veenstra, E. Miller, M. Diaz-Garcia, and A. Heeger, Phys. Rev. B **58**, 7035 (1998).

[7] J. Pollmann and H. Büttner, Phys. Rev. B **16**, 4480 (1977).

[8] M. Matsuura and H. Büttner, Phys. Rev. B **21**, 679 (1980).

[9] N. Harrison, D. Baigent, I. Samuel, R. Friend, A. Grimsdale, S. Moratti, and A. Holmes, Phys. Rev. B **53**, 15 815 (1996).

[10] S. Heun, R. Mahrt, A. Greiner, U. Lemmer, H. Bassler, D. Halliday, D. Bradley, P. Burn, and A. Holmes, J. Phys.: Condens. Matter **5**, 247 (1993).

[11] T.D. Lee, F. Low, and D. Pines, Phys. Rev. B **90**, 297 (1953).

[12] H. Haken, *Quantum Field Theory of Solids: An Introduction* (North-Holland, New York, 1976).

[13] R. Loudon, Am. J. Phys. **27**, 649 (1959).

[14] W.S. Fann and J.H. Hsu, J. Phys. Chem. A **103**, 2375 (1999).

[15] P. Gomes da Costa and E. Conwell, Phys. Rev. B **48**, 1993 (1993).

[16] P. Gomes da Costa, R. Dandra, and E. Conwell, Phys. Rev. B **47**, 1800 (1993).

[17] S. Frolov, W. Gellermann, M. Ozaki, K. Yoshino, and Z. Vardeny, Phys. Rev. Lett. **78**, 729 (1997).

[18] B. Saleh and M. Teich, *Fundamentals of Photonics* (Wiley, New York, 1991).

[19] R. Kersting, U. Lemmer, R. Mahrt, K. Leo, H. Kurz, H. Bässler, and E. Göbel, Phys. Rev. Lett. **70**, 3820 (1993).

[20] M. Yan, L. Rothberg, F. Papadimitritrakopoulos, M. Galvin, and T. Miller, Phys. Rev. Lett. **72**, 1104 (1994).

[21] J. Hsu, M. Yan, T. Jedju, and L. Rothberg, Phys. Rev. B **49**, 712 (1994).

[22] N. Greenham, I. Samuel, G. Hayes, R. Phillips, Y. Kessener, S. Moratti, A. Holmes, and R. Friend, Chem. Phys. Lett. **241**, 89 (1995).

[23] I.D.W. Samuel, G. Rumbles, and C.J. Collison, Phys. Rev. B **52**, R11 573 (1995).